

Heterogeneously Integrated Quantum Chip Interposer Packaging

Ramesh Kudalipalliyalil¹, Sujith Chandran¹, Akhilesh Jaiswal¹, Kang L. Wang², Ajey P. Jacob^{1*}

¹Information Sciences Institute, University of Southern California, Los Angeles, California 90292

²Device Research Laboratory, University of Los Angeles, Los Angeles, California 90095.

*Corresponding author: ajey@isi.edu

Abstract—Quantum computers provide faster solutions to specific compute-intensive classical problems. However, building a fault-tolerant quantum computer architecture is challenging and demands integrating several qubits with optimized signal routing while maintaining its quantum coherence. Experimental realization of such quantum computers with diverse functional components in a planar monolithic device architecture is challenging due to material and thermodynamic mismatch between various elements. Furthermore, it requires complex control and routing, resulting in parasitic modes and reduced qubit coherence. Thus, a scalable interposer architecture is essential to merge and interconnect different functionalities within a sophisticated chip while maintaining qubit coherence. As such, heterogeneous integration is an optimum solution to scale the qubit technology. We propose a heterogeneously integrated quantum chip optoelectronics interposer as a solution to the high-density scalable qubit architecture. Our technology is high-volume manufacturable and provides novel optical I/O solutions for on-chip, chip-to-chip, and cryogenic-to-outside world interconnect.

1. INTRODUCTION

The commercially available quantum computers are either based on superconducting electronics or trapped ions or photonics. Among them, Josephson Junctions based superconducting quantum (SCQ) technology is a promising candidate for scalable quantum computing because of its strong coupling to microwave signals; their limitation is the short coherence lifetime. A fault-tolerant quantum computer architecture demands integrating several qubits with optimized signal routing and control electronics without sacrificing the quantum coherence [1], [2]. Classical interconnects are of large footprint and demands high cooling power. It also undermines the coherency of quantum states by coupling disruptive noises from the environment back into qubits. Also, monolithic integration of such devices is challenging due to the material, and thermodynamic incompatibilities of different quantum components and their increased parasitic modes [3]–[6]. Therefore, a heterogeneously integrated scalable interposer packaging architecture with directional quantum interlink is of great importance to merge and interconnect various functionalities within a sophisticated chip while maintaining qubit coherence. A quantum chip interposer provides tremendous value to the interconnect ecosystem as it helps to provide (1) optimized power, performance, and area benefits, (2) mechanical stability, (3) ease of integrating better thermal dissipating materials through integration architecture optimizations, (4) integrates multiple power/voltage domains (5) can handle fully functional

and versatile test capability. There have been a few efforts recently reported on the interposer level packaging of superconducting qubits [7] and the ion trap qubits [8]. The former, is an electrical interposer architecture and mainly focused on the 3D signal routing and packaging of qubits in cryogenics but not designed to integrate other types of physical qubits, quantum transducer, quantum memory, quantum circulators, etc. Also, these electrical interposers cater to superconducting qubits embedded microwave signals and have limitations in transferring data between the chips (chip-to-chip communication) or from the cryogenic world to the non-cryogenic world. The latter is an optical interposer with bulky optical components which is designed to support only the ion trap qubits and their control/readout optical waveguides.

High fidelity transfer of quantum signals in a non-cryogenic environment is the key bottleneck for networking different quantum computers. For this kind of inter-system connections, quantum converters are needed [9], [10]. For example, superconducting qubits are among the most promising and scalable candidates for implementing nodes in a quantum computing network, and their operation is restricted to cryogenic temperature and microwave frequencies. To coherently exchange quantum states to a different platform will require converting quantum information from microwave to other frequencies, such as optical photons, at which trapped ion/atom systems are operated at. Thus, an essential capability for the networking and development of quantum technology is the interconversion of quantum information between the optical and microwave frequency domains. Recently, Lecocq et al. [11], demonstrated a photonic link-based approach to control and readout the superconducting qubits. In this method, room-temperature microwave signal is electro-optically modulated to the optical domain and routed via optical fibers to the high-speed photodetectors which is integrated with the quantum circuits in the dilution refrigerator.

In this paper, we propose an interposer level packaging scheme, called a quantum chip optoelectronic interposer (QuIP), for the heterogeneous integration of electrical and optical quantum components with high fidelity directional quantum links. Fig. 1 shows the conceptual 2D scheme of the proposed QuIP. The QuIP is analogous integrating a multi-chip module and system-on-a-chip hardware in the classical world [12]. As discussed, the quantum bit interposer will interconnect between two similar or dissimilar quantum bit sources to form (1) an entangled pair or (2) between a quantum

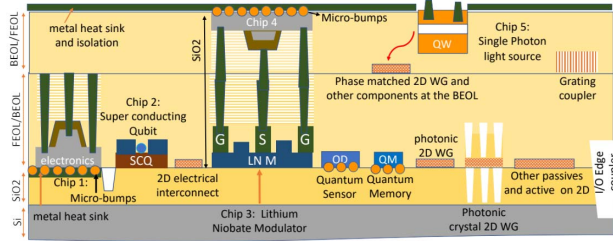
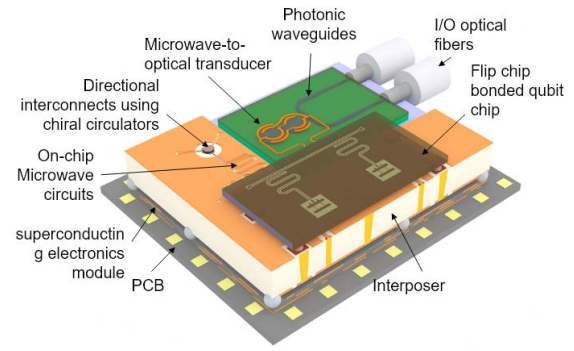


Fig. 1. Conceptual integration scheme of electronic and photonic quantum components in a heterogeneous packaging.

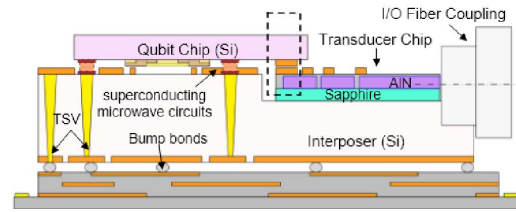
logic unit and a quantum memory unit to store an entangled pair or (3) between a logic unit and a sensor/detector. The quantum chip interposer can also have cryogenic electronic chips to enhance/augment the functions of the quantum chips. As an example, a quantum chip interposer will act as an interconnect between (1) two superconducting quantum bits or (2) two trapped-ion qubits or (3) two P-center qubits or (4) two different quantum bit sources and (5) their associated passive and active components to enhance the functions. The advantage of a quantum bit interposer is that the layout of the interposer's components can be made optimal for its power, performance, and area scaling factors. Thus, the QuIP can be an interface for short-reach or long-reach interconnects. The short reach interconnect will be electrical, and long reach will be optical for data density and power optimization.

The QuIP can improve qubit performance, provide controlled coupling between qubit devices, reduce cross-talk between qubit devices, improve thermal isolation, low microwave loss, and/or substrate mode suppression. The QuIP could also be designed to minimize electromagnetic field leakage. The module architecture can be designed to provide multi-qubit 3-dimensional quantum architectures with individual functional chips in each of the optimum layers. The electronic ICs used for driving the microwave energy to the superconducting chips can be integrated heterogeneously as a flip-chip on another layer with superconducting vias connecting the circuits. The same/dummy vias can also act as heat sinks for signal lines. The same VIA architecture can also be designed to shield quantum circuit from microwaves, for coupling between quantum circuits in different layers and/or for suppressing substrate noise. The interposer can also feature substrates with quantum circuit devices with one operating frequency disposed on a portion of the first surface of the substrate, electrically conducting vias extending through the substrate from the first surface to the second surface, and an electrically conducting [13].

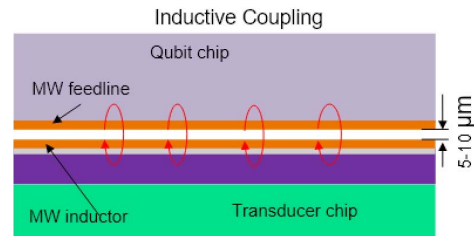
More importantly, the interposer has chiral (unidirectional) links using topological materials or meta-materials that will allow the quantum signals to propagate in a single direction to minimize cross-talks while suppressing environmental disturbances from peripheral control and readout circuitry. This will improve scalability, coherency, and integrability.



(a)



(b)



(c)

Fig. 2. (a) 3D schematic and (b) 2D cross section of the proposed QuIP, (c) illustration of inductive coupling between qubit chip and transducer chip (the dotted rectangle region in (b)).

2. 3D INTEGRATION APPROACH

The Fig. 2 (a) shows the 3D schematic of the proposed QuIP for superconducting qubits with electrical and optical controls. In its simplest form, we have shown only the heterogeneously integrated qubit chip, microwave-to-optical (MO) transducer chip, and on-chip microwave circulators along with electrical, electromagnetic, and optical interconnects on a silicon interposer. The top and bottom side of the interposer is patterned with superconducting micro-strip co-planar waveguides for electrical signal routing, which are interconnected via through-silicon vias (TSVs) [14]. Though silicon is the most compatible platform for qubit integration, microwave electronics, and photonics, integrating qubits on the interposer itself causes electromagnetic interference due to leaky dielectric cladding of the optical waveguides. Moreover, planar integration of the SC qubits on the interposer reduces the scalability. On the other hand, the performance of flip chip bonded qubits has been reported recently in [15], [16] on a silicon platform. We use a similar concept where the qubit chip is flip-chip bonded to the interposer using niobium (Nb)

or indium (In) bonds and electrically connected to the bottom superconducting redistribution layer via TSVs. In the proposed QuIP scheme, the qubit chip shares microwave signals directly with the heterogeneously integrated [17] MO transducer via inductive or capacitive coupling, as shown in the cross-section in Fig. 2(b) and 2(c). We found that the inductive coupling exhibits greater alignment tolerances in the range of 5-10 μm for $> 90\%$ coupling.

A bidirectional transducer converts quantum microwave photons to the optical domain and vice versa [18], [19]. This allows optical quantum communication between different nodes in a quantum network (cryogenic or non-cryogenic). For compact and scalable integration, electro-optic (EO) transducers are widely preferred over other types of MO transducer such as optomechanic, piezo-opto-mechanic, magnonic, etc. Here we propose an EO quantum transducer in the AlN-on-Sapphire platform, which can be heterogeneously integrated on the interposer chip. LiNbO₃-on-insulator (LNOI) is an alternative platform for EO transducer with a large EO coefficient; however, integration of lithium niobate (LN) is relatively complex compared to AlN-on-Sapphire.

Here we propose for the first time the EO transducer (Figs. 3(a)) that is based on two coupled WGM disk resonators (D1 and D2), where one of the disks (D1) is coupled to an input/output bus waveguide. When both the disk resonators have identical intrinsic resonance condition (resonant frequency, $\omega_1 = \omega_2 = \omega_0$ and quality factor, $Q_1 = Q_2 = Q_0$) and strongly coupled, (extrinsic Q factor $Q_c \ll Q_0$), the optical transmission characteristics shows two identical split resonances (Autler-Townes resonance splitting [20]) at ω_l and ω_u , centered at ω_0 . We make use of these split resonance characteristics to design an EO microwave-to-optical frequency converter through non-linear sum frequency generation process as $\omega_u = \omega_l + \Omega_M$, where the optical free spectral range (FSR = $\omega_u - \omega_l$) is detuned to the input microwave frequency Ω_M . Fig. 3(c) (left) shows the optical transmission characteristics of the coupled disk resonator (radius, $R = 30 \mu\text{m}$) designed on a 750 nm thick AlN (EO coefficient $\sim 1 \text{ pm/V}$) on sapphire substrate and 400 nm SiO₂ top cladding. A superconducting (typically Nb or NbN) microwave LC resonator is integrated above the disk resonators where the capacitor electrodes are placed directly on top of the AlN layer (in the slab region as shown in Fig. 3(b)), and the lumped inductor is placed above the SiO₂ cladding connected through vias. The minimum separation between the capacitor electrodes is estimated to be $s = 2.5 \mu\text{m}$, for minimum insertion loss due to mode overlap with the metal and maximum coupling between optical and microwave modes. As mentioned earlier, the microwave resonators are physically isolated and inductively coupled to the qubit chip (see Fig. 2(c)). Fig. 3(c)(right) shows the microwave resonator characteristics near resonance frequency $\Omega_M \sim 6.5 \text{ GHz}$, which is nearly equal to the FSR of the optical spectrum. Additional bias capacitor is also provided to detune the optical characteristics electrically. The loaded optical and microwave Q-factors are calculated to be $Q_{opt} = 1.1 \times 10^5$ and $Q_M = 5900$, respectively. The EO coupling rate g -factor [21] of our device is calculated to be 7.35 kHz ($g/2\pi = 1.17 \text{ kHz}$), assuming the microwave capacitor covers

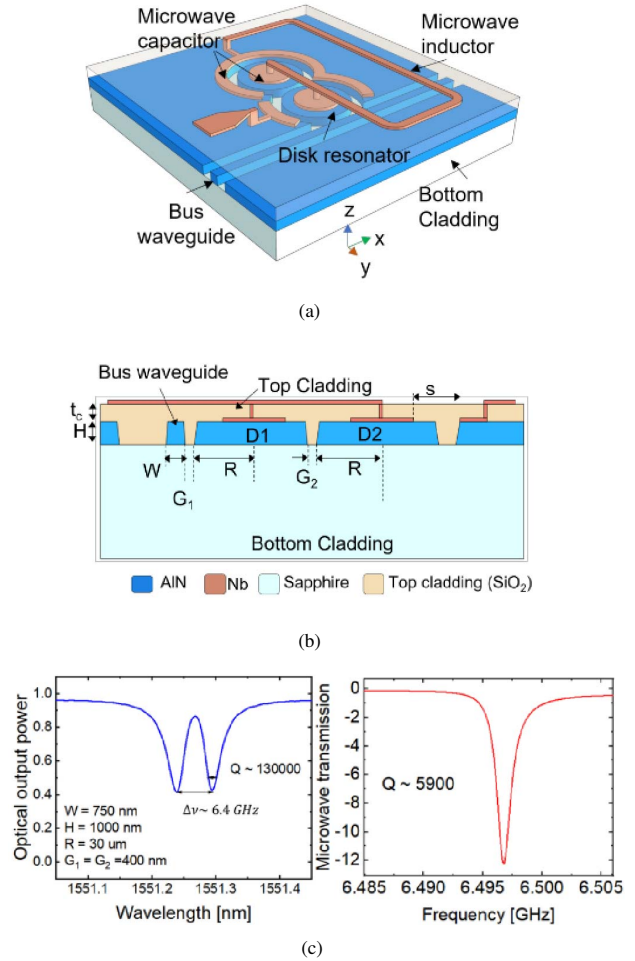


Fig. 3. (a) 3D schematic of the proposed EO frequency transducer based on coupled micro-disk resonators, (b) optical through port transmission characteristics of the EO transducer, (c) microwave resonance characteristics of the superconducting resonator integrated on top of the AlN disk resonators and coupled inductively to the microwave feed line on the qubit chip.

half of the total perimeter of the device. The coupling rate can be further improved by changing the location and geometry of the microwave capacitor electrodes for maximum optical and microwave mode overlap. More details of this device can be seen elsewhere.

Input/output fiber interfacing is another important consideration when operating in cryogenic temperatures. The converted quantum information in the optical domain is coupled to input/output optical fibers and then transported to a cryogenic/non-cryogenic environment for processing. Unlike coupling at room temperature [22], fiber-to-chip coupling in the cryogenic temperature is expected to have very high mechanical and thermal stability. The temperature-dependent expansion or contraction of the adhesive materials might lead to coupling induced loss. In the QuIP scheme we have shown the edge coupler where fiber is mounted in the V-grooves of the Si interposer and aligned with the waveguides in the AlN-on-Sapphire transducer chip. One can also use phase-matched

couplers [23] to couple fibers directly to the Si waveguides (on the interposer) which then evanescently couple to the top transducer waveguides. Due to high wavelength dependency, possible scattering loss, and mechanical instability, grating couplers (coupling from the top of the chip) are expected not a viable solution. Plug-and-play fiber to waveguide coupling

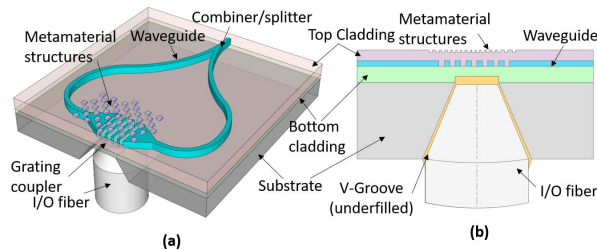


Fig. 4. Schematic (a) 3D view and (b) cross-section of proposed backside optical coupling (BOC) compatible with QuIP.

using 3D funnel structures [24] and fiber-to-chip directional coupling using tapered fibers [25]–[28] are other techniques preferred over conventional edge couplers [29]. Fig. 4 shows a proposed backside optical coupling (BOC) compatible for cryogenic packaging. The BOC technique comprises vertically mounted fiber from the backside of the chip and coupled to the grating couplers (GC) in the device layer with metamaterial structures integrated to eliminate back reflections/substrate-leakage. As a result, the BOC provides better single-photon qubit optical coupling ($<1\text{dB}$ loss), negligible back reflection, and higher mechanical stability for cryogenic quantum chip applications. More details on this work will be available elsewhere.

The interposer chip is also compatible for integrating on-chip microwave quantum Hall circulators which are 1000 times smaller than conventional nonreciprocal 3D cavity circulators based on ferrite devices [30], [31]. Recently, Martinez et al. reported [31] a micron-sized cryogenic non-reciprocal circulator based on topological materials that exhibits more than 20 dB isolation at the fundamental plasmon frequency $f = 0.65$ GHz and over a bandwidth of ~ 160 MHz. Such directional interconnects are highly demanded for a fault tolerant machine to increase the coherence time and reduce the error rate below the threshold value for quantum error correction. Inserting magnetic material into photonic crystals breaks the time reversal symmetry and induce chiral edge modes for optical photons. Such chiral optical interconnects will be beneficial for photonic and cold-atom quantum systems, as well as long-haul quantum networks exploiting telecom bandwidth.

Fig. 5 shows a typical QuIP integration flow. Again, the assumption is that the functional chips are already fabricated and brought together for integrating on the interposer. However, there are patterning and integration challenges that must be addressed to envisage a functional interposer circuit to interconnect these chips. Besides, the assembly, test, fiber, laser connections, electrical inputs shall add to the complexity of deployment of the interposer. These challenges will become increasingly significant as more qubits and functionally diverse

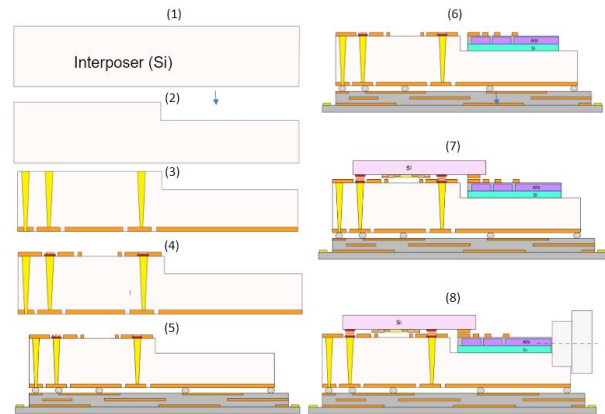


Fig. 5. Integration process flow for the proposed QuIP. The edge coupling scheme is shown for illustration. (1) Interposer material (Si), (2) recessed region and V-groove fabrication, (3) TSV fabrication, (4) patterning of microwave circuits on the interposer, (5) transducer chip bonding, (7) bonding of SC qubit chip, circulator chip, etc., (8) fiber coupling and alignment.

elements are integrated on the interposer. Some apparent challenges include solutions to address thermal and electromagnetic isolations when various functional devices are integrated together.

In addition, clever and disruptive packaging approaches that address the design-for-manufacturing cost targets require to be implemented to address not just the integration scheme but also the optical (fiber to laser and laser to die) and electrical I/O.

The starting material for the interposer flow is silicon. The reason for using silicon is its cryogenic characteristics, ease of designing an I/O scheme and negligible microwave dielectric loss as compared to other substrates like sapphire and silicon dioxide. Moreover, thick silicon interposer region isolates the qubits from electromagnetic interference from the bottom circuits. The silicon substrate is now prepared through patterning to integrate various functional devices, including superconducting junction, transducer elements, and photonics waveguides. The silicon substrate is then thinned and polished to fabricate TSVs, a standard process. The TSV process can also be a last step in the interposer flow. Based on the optical I/O integration schemes, either a backside V-groove coupler or an adiabatic coupler will be designed on the interposer. Following the patterning of functional regions, each of these functional chips is separately integrated onto the substrate either using electrostatic bonding or metal to metal fusion bonding process schemes. For example, as shown in Fig. 5, the transducer chip is first bonded to the interposer and then the qubit chip is flip chip bonded while aligning the feedlines to the transducer chip (see Fig. 2). In the final stage the chip is wire bonded and input/output fibers are connected. The chip is then packaged in a cryogenic housing with proper thermalization and electromagnetic shielding [7], [32], [33].

3. CONCLUSION

Heterogeneous integration of disaggregated hardware on an interposer can create a multifunction module to bring a whole new perspective to fault tolerant quantum information

processing implementation. We present the concept and implementation scheme for a novel quantum chip optoelectronics interposer (QuIP) that will serve as an interface between multiple components and chiplets of the same or different functions to create such a quantum module on an integrated chip for the first time. The interconnects between these components can be either electrical or optical waveguides. The inter-chip inductive coupling provides better alignment tolerance (5-10 μm) for bonding qubit chips onto the interposer. While the electrical interconnects are suitable for short reach, photonics waveguides on the interposer can bring chip-to-chip or dewar to dewar or long reach quantum data transfer. Our preliminary simulation results of the proposed AlN-based EO transducer show that the quantum conversion rate (g) can be as high as 7.35 KHz and the overall footprint is 2 times smaller than the recently demonstrated devices. In practice, the performance of this device can be further improved with optimized device dimensions and advanced low-loss waveguide fabrication techniques. Furthermore, the proposed integration scheme is compatible for integrating chiral interconnects using topological materials which are recently found attractive for unidirectional quantum information transfer. In conclusion, the QuIP, as a heterogeneous packaging, mix and match different quantum components in different fabrication technologies with improved RF performance and enables networking of fault tolerant quantum computers inside the cryogenic, as well as cryogenic-to-outside world.

ACKNOWLEDGMENT

This material is based upon work supported by the National Science Foundation under the Convergence Accelerator Research program Grant No. 2040737.

REFERENCES

- [1] A. Fruchtmann and I. Choi, "Technical roadmap for fault-tolerant quantum computing," *NQIT Technical Roadmap*, 2016.
- [2] D. Awschalom, K. K. Berggren, H. Bernien, S. Bhavne, L. D. Carr, P. Davids, S. E. Economou, D. Englund, A. Faraon, M. Fejer *et al.*, "Development of quantum interconnects (quics) for next-generation information technologies," *PRX Quantum*, vol. 2, no. 1, p. 017002, 2021.
- [3] Q. Liu, M. Li, K. Dai, K. Zhang, G. Xue, X. Tan, H. Yu, and Y. Yu, "Extensible 3d architecture for superconducting quantum computing," *Applied Physics Letters*, vol. 110, no. 23, p. 232602, 2017.
- [4] J. Béjanin, T. McConkey, J. Rinehart, C. Earnest, C. McRae, D. Shiri, J. Bateman, Y. Rohanizadegan, B. Penava, P. Breul *et al.*, "Three-dimensional wiring for extensible quantum computing: The quantum socket," *Physical Review Applied*, vol. 6, no. 4, p. 044010, 2016.
- [5] S. Pauka, K. Das, R. Kalra, A. Moini, Y. Yang, M. Trainer, A. Bousquet, C. Cantaloube, N. Dick, G. Gardner *et al.*, "A cryogenic cmos chip for generating control signals for multiple qubits," *Nature Electronics*, vol. 4, no. 1, pp. 64–70, 2021.
- [6] J. C. Adcock, J. Bao, Y. Chi, X. Chen, D. Bacco, Q. Gong, L. K. Oxenløwe, J. Wang, and Y. Ding, "Advances in silicon quantum photonics," *IEEE Journal of Selected Topics in Quantum Electronics*, vol. 27, no. 2, pp. 1–24, 2020.
- [7] D.-R. W. Yost, M. E. Schwartz, J. Mallek, D. Rosenberg, C. Stull, J. L. Yoder, G. Calusine, M. Cook, R. Das, A. L. Day *et al.*, "Solid-state qubits integrated with superconducting through-silicon vias," *npj Quantum Information*, vol. 6, no. 1, pp. 1–7, 2020.
- [8] M. H. Devoret and R. J. Schoelkopf, "Superconducting circuits for quantum information: an outlook," *Science*, vol. 339, no. 6124, pp. 1169–1174, 2013.
- [9] S. Krastanov, H. Raniwala, J. Holzgrafe, K. Jacobs, M. Lončar, M. J. Reagor, and D. R. Englund, "Optically heralded entanglement of superconducting systems in quantum networks," *Physical Review Letters*, vol. 127, no. 4, p. 040503, 2021.
- [10] N. Lauk, N. Sinclair, S. Barzanjeh, J. P. Covey, M. Saffman, M. Spiropulu, and C. Simon, "Perspectives on quantum transduction," *Quantum Science and Technology*, vol. 5, no. 2, p. 020501, 2020.
- [11] F. Lecocq, F. Quinlan, K. Cicak, J. Aumentado, S. Diddams, and J. Teufel, "Control and readout of a superconducting qubit using a photonic link," *Nature*, vol. 591, no. 7851, pp. 575–579, 2021.
- [12] B. Sirbu, Y. Eichhammer, H. Oppermann, T. Tekin, J. Kraft, V. Sidorov, X. Yin, J. Bauwelinck, C. Neumeier, and F. Soares, "3d silicon photonics interposer for tb/s optical interconnects in data centers with double-side assembled active components and integrated optical and electrical through silicon via on soi," in *2019 IEEE 69th Electronic Components and Technology Conference (ECTC)*. IEEE, 2019, pp. 1052–1059.
- [13] C. Thomas, J. Charbonnier, A. Garnier, N. Bresson, F. Fournel, S. Renet, R. Franiatte, N. David, V. Thiney, M. Urdampilleta *et al.*, "Die-to-wafer 3d interconnections operating at sub-kelvin temperatures for quantum computation," in *2020 IEEE 8th Electronics System-Integration Technology Conference (ESTC)*. IEEE, 2020, pp. 1–7.
- [14] M. Vahidpour, W. O'Brien, J. T. Whyland, J. Angeles, J. Marshall, D. Scarabelli, G. Crossman, K. Yadav, Y. Mohan, C. Bui *et al.*, "Superconducting through-silicon vias for quantum integrated circuits," *arXiv preprint arXiv:1708.02226*, 2017.
- [15] K. Satzinger, C. Conner, A. Bienfait, H.-S. Chang, M.-H. Chou, A. Cleland, E. Dumur, J. Grebel, G. Peairs, R. Povey *et al.*, "Simple non-galvanic flip-chip integration method for hybrid quantum systems," *Applied Physics Letters*, vol. 114, no. 17, p. 173501, 2019.
- [16] D. Rosenberg, D. Kim, R. Das, D. Yost, S. Gustavsson, D. Hover, P. Krantz, A. Melville, L. Racz, G. Samach *et al.*, "3d integrated superconducting qubits," *npj quantum information*, vol. 3, no. 1, pp. 1–5, 2017.
- [17] M. A. Schmidt, "Wafer-to-wafer bonding for microstructure formation," *Proceedings of the IEEE*, vol. 86, no. 8, pp. 1575–1585, 1998.
- [18] X. Han, W. Fu, C.-L. Zou, L. Jiang, and H. X. Tang, "Microwave-optical quantum frequency conversion," *Optica*, vol. 8, no. 8, pp. 1050–1064, 2021.
- [19] W. Hease, A. Rueda, R. Sahu, M. Wulf, G. Arnold, H. G. Schwefel, and J. M. Fink, "Bidirectional electro-optic wavelength conversion in the quantum ground state," *PRX Quantum*, vol. 1, no. 2, p. 020315, 2020.
- [20] B. Li, C. P. Ho, and C. Lee, "Tunable autler-townes splitting observation in coupled whispering gallery mode resonators," *IEEE Photonics Journal*, vol. 8, no. 5, pp. 1–10, 2016.
- [21] A. Rueda, F. Sedlmeir, M. C. Collodo, U. Vogl, B. Stiller, G. Schunk, D. V. Strekalov, C. Marquardt, J. M. Fink, O. Painter *et al.*, "Efficient microwave to optical photon conversion: an electro-optical realization," *Optica*, vol. 3, no. 6, pp. 597–604, 2016.
- [22] L. T. Guan, L. H. Yu, J. M. Chinq, E. W. L. Ching, C. S. Choong, L. S. Thor, T. Y. Ang, and O. J. Rong, "Silicon optical electrical interposer-fiber to the chip," in *2019 IEEE 21st Electronics Packaging Technology Conference (EPTC)*. IEEE, 2019, pp. 34–39.
- [23] Y. Bian, A. Jacob, A. Thomas, B. Peng, M. Rakowski, W. S. Lee, and R. Augur, "Light manipulation in a monolithic silicon photonics platform leveraging 3d coupling and decoupling," in *Frontiers in Optics*. Optical Society of America, 2020, pp. FTu6E–3.
- [24] O. A. J. Gordillo, S. Chaitanya, Y.-C. Chang, U. D. Dave, A. Mohanty, and M. Lipson, "Plug-and-play fiber to waveguide connector," *Optics express*, vol. 27, no. 15, pp. 20305–20310, 2019.
- [25] T. Carmon, S. Y. Wang, E. P. Ostby, and K. J. Vahala, "Wavelength-independent coupler from fiber to an on-chip cavity, demonstrated over an 850nm span," *Optics express*, vol. 15, no. 12, pp. 7677–7681, 2007.
- [26] M. Davanço and K. Srinivasan, "Efficient spectroscopy of single embedded emitters using optical fiber taper waveguides," *Optics express*, vol. 17, no. 13, pp. 10542–10563, 2009.
- [27] A. W. Schell, H. Takashima, T. T. Tran, I. Aharonovich, and S. Takeuchi, "Coupling quantum emitters in 2d materials with tapered fibers," *ACS Photonics*, vol. 4, no. 4, pp. 761–767, 2017.
- [28] S. Khan, S. M. Buckley, J. Chiles, R. P. Mirin, S. W. Nam, and J. M. Shainline, "Low-loss, high-bandwidth fiber-to-chip coupling using capped adiabatic tapered fibers," *APL Photonics*, vol. 5, no. 5, p. 056101, 2020.
- [29] R. Marchetti, C. Lacava, L. Carroll, K. Gradkowski, and P. Minzioni, "Coupling strategies for silicon photonics integrated chips," *Photonics Research*, vol. 7, no. 2, pp. 201–239, 2019.
- [30] A. Mahoney, J. Colless, S. Pauka, J. Hornibrook, J. Watson, G. Gardner, M. Manfra, A. Doherty, and D. Reilly, "On-chip microwave quantum hall circulator," *Physical Review X*, vol. 7, no. 1, p. 011007, 2017.

- [31] L. Martinez, G. Qiu, G. Carosi, K. Wang, J. DuBois, and D. Qu, "Non-reciprocal microwave devices with a topological material," *Bulletin of the American Physical Society*, 2022.
- [32] R. N. Das, J. Yoder, D. Rosenberg, D. Kim, D. Yost, J. Mallek, D. Hover, V. Bolkhovsky, A. Kerman, and W. Oliver, "Cryogenic qubit integration for quantum computing," in *2018 IEEE 68th Electronic Components and Technology Conference (ECTC)*. IEEE, 2018, pp. 504–514.
- [33] B. Lienhard, J. Braumüller, W. Woods, D. Rosenberg, G. Calusine, S. Weber, A. Vepsäläinen, K. O'Brien, T. P. Orlando, S. Gustavsson *et al.*, "Microwave packaging for superconducting qubits," in *2019 IEEE MTT-S International Microwave Symposium (IMS)*. IEEE, 2019, pp. 275–278.